Journal of ELECTRONIC MATERIALS, Vol. 41, No. 3, 2012
DOI: 10.1007/s11664-011-1823-6


# Synthesis of Vertically Aligned ZnO Nanorods on Ni-Based Buffer Layers Using a Thermal Evaporation Process

DONG-HAU KUO,[1,3] JHENG-YU HE,[1] and YING-SHENG HUANG[2]

1.—Department of Materials Science and Engineering, National Taiwan University of Science and Technology, Taipei 10607, Taiwan. 2.—Department of Electrical Engineering, National Taiwan University of Science and Technology, Taipei 10607, Taiwan. 3.—e-mail: dhkuo@mail.ntust.edu.tw

Uniform, vertically aligned ZnO nanorods have been grown mainly on Au-coated and ZnO-coated sapphire substrates, ZnO- and GaN-coated substrates, or self-catalyzing substrates. Conventionally, Ni-coated substrates have resulted in thick rods with diameter more than 250 nm, rods with non-uniform distribution in diameter, or rods with an alignment problem. In the best result in this paper, slender, uniform, vertically aligned, solely UV-emitting ZnO nanorods with diameter of 110 ± 25 nm and length of 30 ± 10 $\mu$m have been successfully grown at 700°C for 2 h on sapphire substrates covered with Ni-based buffer layers by using metallic zinc and oxygen as reactants. Scanning electron microscopy and room-temperature photoluminescence have been used to investigate the effects of process conditions on the slenderness and vertical alignment of the ZnO rods. To develop the desired ZnO nanorods, etched sapphire substrates, a second metallic Sn buffer layer on top of a spin-coated nickel oxide layer, polyvinyl alcohol binder at 10% concentration in solution of iron nitrate, and pyrolysis and reduction reactions were involved. Defect photoemission for thick ZnO rods is attributed to insufficient oxygen supply during the growth process with fixed oxygen flow rate.

**Key words:** Nanostructure, ZnO, nanomaterials, semiconducting materials

## INTRODUCTION

Zinc oxide (ZnO) with a wide band gap of 3.37 eV and large exciton binding energy (60 meV) has become of great interest due to its importance in basic scientific research and potential technological applications.[1–3]

Vertically aligned ZnO nanorods with different diameters have been synthesized by chemical vapor deposition, solution methods, evaporation, etc. with or without catalysts on various substrates. One-dimensional (1-D) ZnO arrays also have been grown by a low-temperature hydrothermal method at <100°C with a ZnO buffer layer on various substrates.[4,5] Uniform, vertically aligned ZnO nanorods with slender diameter of 50 nm to 150 nm have been demonstrated by using the carbothermal reaction between ZnO and carbon black above 850°C on Au catalyst-patterned sapphire substrates with the aid of submicrometer-sized polystyrene balls[6] and laser-hardening lithography technology.[7,8] Well-aligned 1-D ZnO grown with a metallic Zn reactant by thermal evaporation at 750°C to 850°C on GaN- or ZnO-covered sapphire substrates has been reported.[9,10] The keys to successful growth of uniform, aligned ZnO nanorods by gas-phase reactions are the use of sapphire substrates and buffer layers on the substrate. Buffer layers of Au, Sn,[11–13] Ni,[14] Cu,[15] etc. and a self-catalyzing ZnO layer[9,16,17] have been applied. Au, GaN, and ZnO have been recognized as the most effective materials for buffer layers. Umar et al.[14] grew hexagonal-shaped ZnO rods with larger diameter of 300 nm to 350 nm on Ni-coated substrates at 500°C to 550°C using Zn powders in an oxygen atmosphere. Their nickel buffer layer led to 1-D ZnO with larger diameter but showed a uniformity problem, with rod

(Received June 27, 2011; accepted November 14, 2011; published online December 2, 2011)

diameter ranging from 60 nm to 120 nm[9,14] or from 40 nm to 250 nm.[10] Therefore, growth of vertically aligned ZnO nanorods with uniform size distribution by using metallic Zn as a reactant on Ni-based buffer layer-covered sapphire substrates is a challenge. In this study, we demonstrate slender, uniform, vertically aligned ZnO nanorods with diameter of ~110 nm on Ni-based buffer layer-covered sapphire substrates.

## EXPERIMENTAL PROCEDURES

ZnO nanowires were grown at 700°C for 2 h on buffer layer-coated Si wafers or sapphire substrates by a thermal evaporation process under a mixture flow of 10 standard cubic centimeters per minute (sccm) $O_2$ and 200 sccm $N_2$ with a mixture source of Zn and ZnO at weight ratio (g) of 1.0:1.0. The preparation of the buffer layers involved two methods: spin coating and direct-current (DC) sputtering. The spin coatings of single Ni and mixed (Sn + Ni) and (In + Ni) layers utilized 0.01 M solutions of nickel nitrate, zinc nitrate, or tin chloride, followed by pyrolysis at 650°C for 30 min and a reduction reaction at 850°C for 30 min in a (Ar + 7% $H_2$) mixed gas. The coating solution contained 1 wt.%, 5 wt.%, 10 wt.%, or 20 wt.% polyvinyl alcohol (PVA). For DC sputtering, Ni and Sn films were deposited at output powers of 70 W and 20 W, respectively, for 1 min. Au catalyst films also were deposited for comparison. These sputtered layers had thickness of 30 nm to 60 nm. In addition to single and mixed buffer layers, Sn/Ni bilayers also were prepared on sapphire substrates etched with 0.1 M NaOH solution for 15 s or without etching. The formation of a Sn/Ni buffer bilayer involved spin coating with Ni nitrate solution, pyrolizing to from NiO, sputter-depositing Sn metal on NiO, and finally executing a reduction reaction. Scanning electron microscopy (SEM) was used to observe the growth morphology. Phase identification and microstructural characterization of nanorods were conducted by transmission electron microscopy (TEM). Room-temperature photoluminescence (PL) measurements were performed using a 325-nm He-Cd laser as excitation source.

## RESULTS AND DISCUSSION

Figure 1 shows surface morphologies of 1-D ZnO grown at 700°C for 2 h on (a) Ni sputter-coated and (b) Ni spin-coated Si substrates and on (c) Ni spin-coated and (d) Au sputter-coated sapphire substrates by thermal evaporation with a mixture source of Zn and ZnO at weight ratio (g) of 1.0:1.0. One-dimensional ZnO materials grown on Ni spin-coated Si wafer substrates were inclined and had hexagonal cross-section with size of 800 nm to 1.5 $\mu$m, while those on Ni sputter-coated substrates had leaf-like shape with cross-sectional size of 600 nm to 1.2 $\mu$m. Spin-coated Ni layers after pyrolysis and the reduction reaction can favor growth of ZnO rods with hexagonal cross-section. When the Si substrates with a Ni spin-coated layer were replaced by Ni-coated, (0001)-oriented sapphire substrates, the vertical alignment of the grown ZnO rods was greatly improved while maintaining the larger diameter of 2 $\mu$m to 3 $\mu$m (Fig. 1c). Au has been the

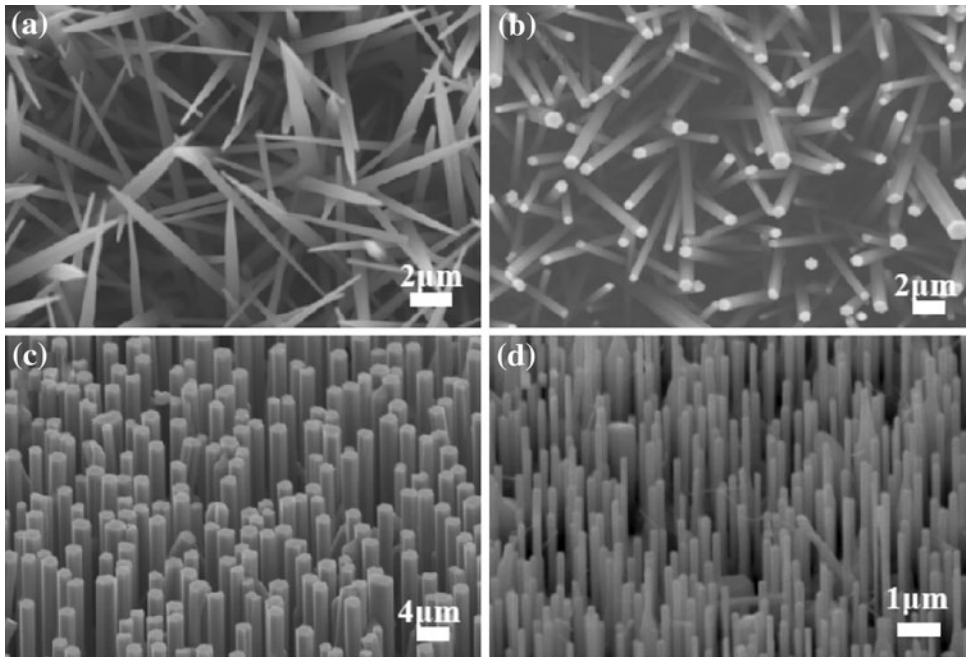


Fig. 1. Surface morphologies of 1-D ZnO grown at 700°C for 2 h on (a) Ni sputter-coated and (b) Ni spin-coated Si substrates and on (c) Ni spin-coated and (d) Au sputter-coated sapphire substrates by thermal evaporation with a mixture source of Zn and ZnO at weight ratio (g) of 1.0:1.0. The 0.01 M nitrate spin solution contained 1% PVA.

most popular catalyst for growing 1-D ZnO. With the same growth condition, vertically aligned ZnO nanorods with diameter of 200 nm were easily obtained on Au-covered substrates, as shown in Fig. 1d. However, growth of ZnO rods with diameter of 100 nm is obviously a challenge.

To make slender ZnO rods, different PVA concentrations were added to the spin-coating solutions for the purpose of preventing the deposited buffer layers from clustering after pyrolysis and reduction. It is expected that, as the nickel nitrate content becomes comparatively less at higher PVA concentration, the pyrolized NiO films will be thinner and the reduced Ni catalyst particles will be smaller. Figure 2 shows surface morphologies of 1-D ZnO grown with 0.01 M solutions of nickel nitrate mixed with (a) 5%, (b) 10%, and (c) 20% PVA. When the PVA concentration increased to 5%, a few ZnO rods had smaller diameter of 200 nm to 300 nm but most of rods still had diameter of 2 $\mu$m to 3 $\mu$m. At 10% PVA, most of the ZnO rods had diameter of 200 nm to 300 nm, but intermixed with some thick rods of 1 $\mu$m to 2 $\mu$m diameter. When the PVA concentration reached 20%, the alignment and crystallinity (as determined by x-ray diffraction intensity) of the ZnO rods with diameter of 2 $\mu$m were degraded. The optimal PVA concentration was found to be 10% in order to form rods that were still vertically aligned but were slender. Our reduced Ni catalyst particles were covered by a Zn vapor during the heating stage. Reactions between Ni and Zn occurred. When the growth temperature reached 700°C, oxygen entered and oxidized the covering Zn/Ni layer to grow the ZnO rods. The metal-embedded buffer layers can generate a strain state. At the condition of 10% PVA, the buffer layer reached a better strain state for growing rods of smaller size and better alignment. To further improve nucleation on the buffer layer for growing 1-D ZnO, sapphire substrates were chemically etched with 0.1 M NaOH solution.[18] Figure 2d shows 1-D ZnO grown on etched sapphire substrates on which a spin-coated Ni buffer layer had been covered. Comparing Fig. 2c and Fig. 2d, the diameters of the ZnO rods changed from 200 nm to 2 $\mu$m to become 100 nm to 400 nm after sapphire substrates were etched. By using the substrate-etching approach, ZnO nanorods were thinned while still keeping the rods vertically aligned.

To further reduce the diameter of the ZnO rods to nanoscale, a second component was added to the Ni buffer layer covered on the sapphire substrates. Figure 3 shows the surface morphologies of ZnO rods grown on (a) (Sn + Ni) and (b) (In + Ni) spin-coated and etch-free sapphire substrates. These spin-coating solutions contained 10% PVA. The addition of Sn to the Ni for the buffer layer helped to form uniform, vertically aligned ZnO nanorods, but the rods for the (In + Ni) system now lay down on the substrate. Both of the systems produced ZnO nanorods of 200 nm diameter. Although a few ZnO crystals were observed (Fig. 3a), most of the ZnO rods were vertically aligned and slender, having quite uniform diameter of 200 nm. Prior to the addition of a second component, our growth of 1-D ZnO still exhibited a problem with diameter uniformity. However, the addition of Sn favored thinning and the uniformity of the ZnO rods. Based

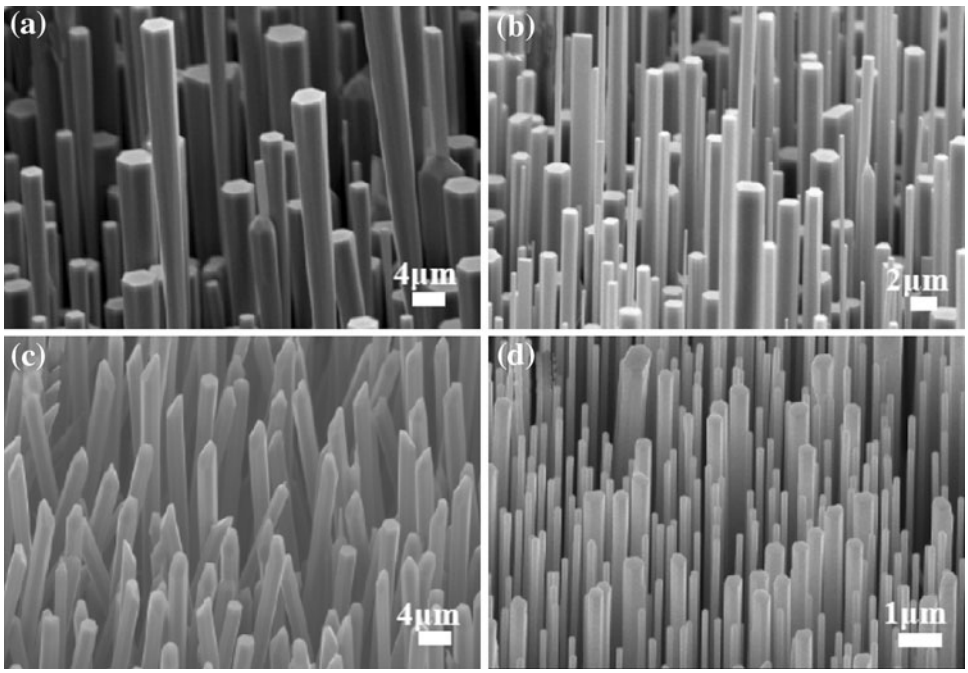


Fig. 2. Surface morphologies of 1-D ZnO grown at 700°C for 2 h on sapphire substrates spin coated with 0.01 M solution of nickel nitrate mixed with (a) 5%, (b) 10%, and (c) 20% PVA or on (d) NaOH-etched sapphire substrates spin coated with nickel nitrate solution containing 10% PVA.

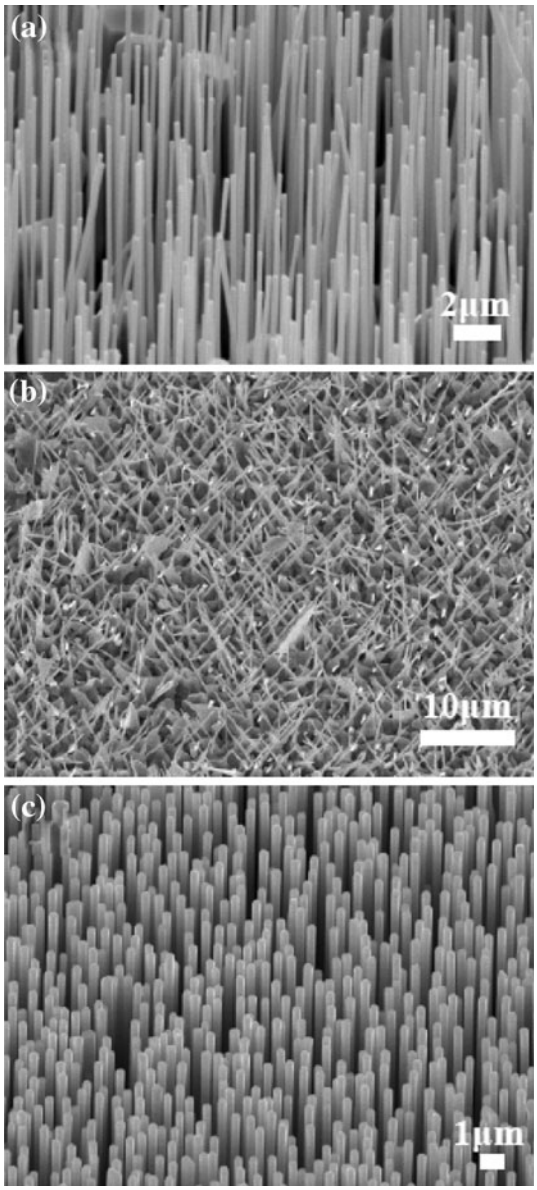


Fig. 3. Surface morphologies of ZnO rods grown at 700°C for 2 h on (a) (Sn + Ni) and (b) (In + Ni) spin-coated and on (c) Sn sputter/Ni spin-coated sapphire substrates without NaOH etching.

upon the binary phase diagram, the buffer layer for the (Sn + Ni) system after a reduction reaction formed a $Ni_3Sn_2$ compound with an incongruent melting temperature of 1260°C. For the (In + Ni) system, pyrolysis at 650°C formed a (Ni + $In_2O_3$) buffer layer. $In_2O_3$, which has a melting temperature of 850°C and starts to volatize at 850°C, was expected to be reduced at 850°C to form the (In-Ni) compound with melting point of ~910°C. The formation of different compounds leads to different degrees of stiffness of the buffer layer at growth temperature of 700°C. The (In-Ni) compound becomes softer and cannot provide a stiff buffer layer, therefore the grown ZnO rods tend to lie down on the sapphire substrate. In general, the second components of Sn and In together with Ni can lead to uniform and slender ZnO nanorods. Due to our focus on vertical alignment, the mixed (Sn + Ni) system instead of the (In + Ni) system was chosen in a bilayer configuration, denoted herein as the Sn sputter/Ni spin-coated or briefly the Sn/Ni system. Figure 3c shows a SEM image of 1-D ZnO grown on Sn sputter/Ni spin-coated sapphire substrates without NaOH etching. One-dimensional ZnO grown on the Sn/Ni bilayer system was vertically aligned, had uniform diameter of 400 nm, and was free of observed ZnO crystals. Therefore, the major advantage of using Sn in the Sn/Ni system is to improve the diameter uniformity of the ZnO rods.

The Sn/Ni-catalyzed growth of 1-D ZnO in Fig. 3c was further improved by using NaOH-etched sapphire substrates. Figure 4 shows (a) low- and (b) high-magnification SEM images of ZnO nanorods grown on Sn/Ni-coated and NaOH-etched sapphire substrates. Uniform, flat-ended, vertically aligned ZnO nanorods with diameter of $110 \pm 25$ nm and hexagonal cross-sectional shape were successfully synthesized. Our ZnO nanorods had long length of $30 \pm 10$ $\mu$m. There were no droplets attached to rod tips, indicating that growth did not follow the vapor–liquid–solid growth mechanism. Figure 4 also displays (c) a high-resolution TEM image and (d) a diffraction pattern by TEM analysis for the ZnO nanorod shown inset to Fig. 4c. The electron diffraction pattern in Fig. 4d from the ZnO nanorod shown inset to Fig. 4c was helpful to identify its crystal structure as a hexagonal wurtzite phase with [−110] zone diffraction pattern. The (002) lattice fringe of a Sn/Ni-catalyzed ZnO nanorod in Fig. 4c had lattice spacing of 0.521 nm, close to that of pure ZnO at 0.5209 nm. This similar spacing indicates the purity of our ZnO rods. The growth direction (shown by an arrow in the inset to Fig. 4c) was identified to be the *c* axis.

Figure 5 displays the room-temperature photoluminescence spectra of vertically aligned, *c*-axis-oriented ZnO rods with (a) large (2 $\mu$m to 3 $\mu$m, Fig. 1c), (b) medium (400 nm, Fig. 3c), and (c) small (110 nm, Fig. 4a) diameter. A sharp, strong photoemission peak at 383 nm to 387 nm (3.23 eV to 3.20 eV) was obtained for ZnO rods with different diameters. This sharp peak corresponds to the near-band-edge peak. Full-width at half maximum (FWHM) in intensity was 140 meV, 150 meV, and 150 meV for the excitonic emissions from rods with large, medium, and small diameter, respectively. Our small FWHM values for ZnO rods with different diameters indicate their good crystallinity. Furthermore, broadband green emission centered at 510 nm to 512 nm (2.43 eV to 2.42 eV) was observed due to the lattice defects in 1-D ZnO with larger diameters.

Only 1-D ZnO rods with small diameter of 110 nm did not show green emission. From the photoluminescence results, the ZnO rods with small diameter had good crystallinity and were pure without

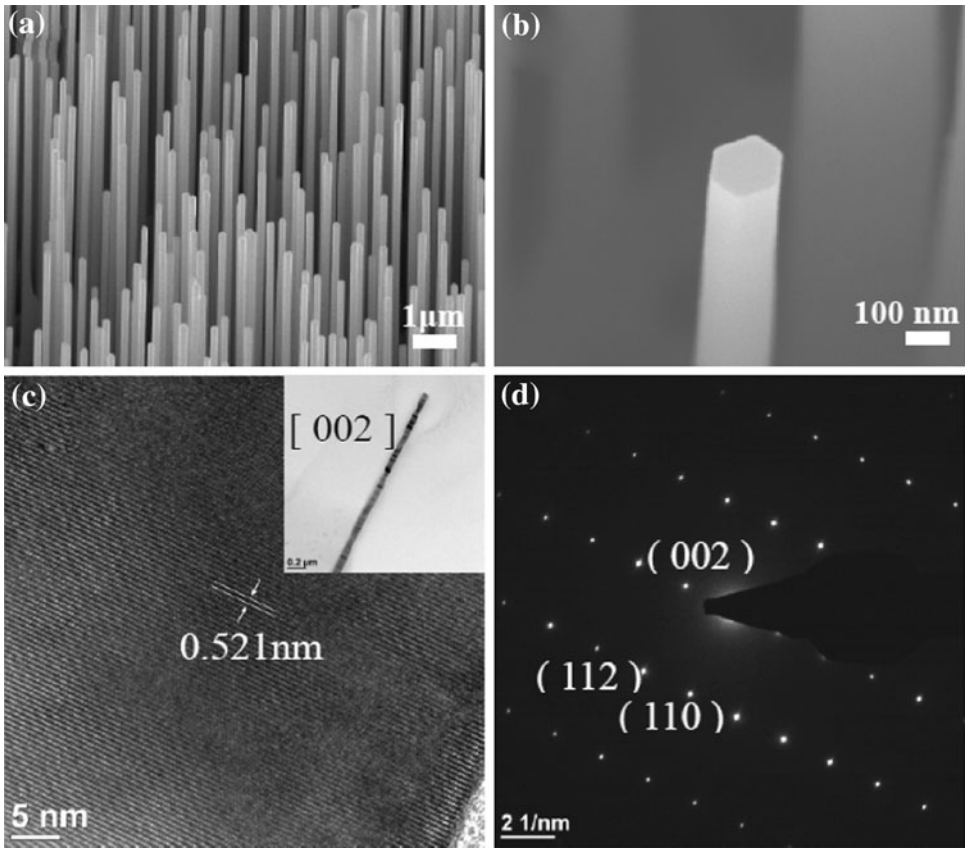


Fig. 4. (a) Low- and (b) high-magnification SEM images of ZnO nanorods grown at 700°C for 2 h on Sn sputter/Ni spin-coated sapphire substrates etched with 0.01 M NaOH solution for 15 s. (c) Lattice image and (d) diffraction pattern of TEM analyses for the ZnO nanorods shown inset to (c).

Sn doping. The intensity of the green emission was stronger for 1-D ZnO with larger diameter. During our ZnO growth, the process parameters, including the oxygen flux, were kept constant. However, the thick rods need more oxygen to react with the Zn vapor. If the oxygen supply is just sufficient for slender rods, then the thick rods may be oxygen deficient, resulting in oxygen vacancies. The green luminescence at ~2.5 eV is attributed to the bulk defects of oxygen vacancies.[19,20] Intrinsic defects of ionic compounds involve Schottky and Frenkel defects. From the Brouwer diagram, the major defects under the oxygen-deficient condition are oxygen vacancies and bound electrons.[21] Our photoluminescence results also demonstrate that our reaction chamber does not have a leakage problem. Chang et al.[22] reported a similar situation for thick rods, with green emission. Shalish et al.[23] reported the opposite results. When the size effect of 1-D ZnO is investigated, the process conditions and the control of oxygen pressure in the growth chamber need to be carefully considered. Additionally, a small, broad feature of red luminescence located at 1.97 eV (629.6 nm) can be attributed to the transition from the conduction band to the defect level of oxygen interstitials caused by incomplete atomic packing resulting from the growth from vapor.[24]

Uniform, vertically aligned, slender ZnO nanorods were successfully grown by different approaches by modifying the buffer layer or adjusting the nucleation mechanism on treated substrates. A single Ni catalyst layer on a substrate cannot lead to uniform, slender ZnO nanorods. A metallic Sn layer to alloy with the underlying Ni species is advantageous for growth of the expected nanorods. The bilayer Sn/Ni alloy will be covered with Zn vapor before oxygen enters the reaction chamber, as the growth temperature reaches 700°C. The Zn covering layer reacts with the Sn/Ni alloy. Once this Zn covering layer has oxidized, its reaction with the Sn/Ni alloy will stop. The resulting ZnO covering layer will be embedded with Sn/Ni-related nanoparticles. For growth of ZnO nanorods on Ni-covered substrates, the ZnO covering layer will also be embedded with Ni-related nanoparticles. Apparently, addition of a Sn component to the Ni-based buffer layer changes the nucleation mechanism in favor of growth of uniform, aligned, slender ZnO nanorods.

## CONCLUSIONS

Uniform, vertically aligned ZnO nanorods grown with Ni-based buffer layers at 700°C for 2 h on (0001)-oriented sapphire substrates were successfully

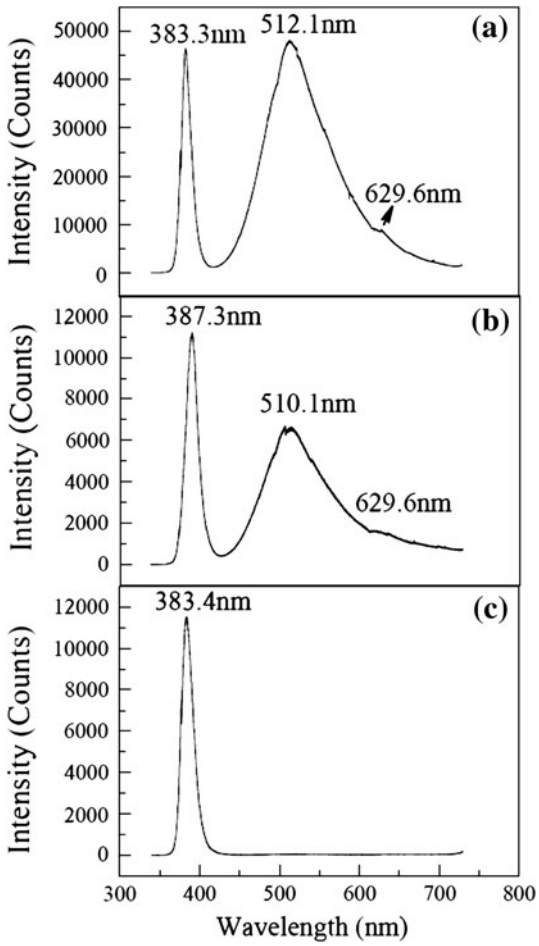


Fig. 5. Photoluminescence spectra of vertically aligned ZnO rods with (a) large (2 $\mu$m to 3 $\mu$m), (b) medium (400 nm), and (c) small (110 nm) diameter.

synthesized. To overcome problems regarding diameter size, diameter uniformity, and rod alignment, we developed an approach to obtain slender, long, uniform, vertically aligned, solely UV-emitting ZnO nanorods, which involves coating techniques, substrate selection, binder usage, and second components. Addition of the second component Sn enables ZnO nanorods of uniform diameter to be obtained. The spin-coated NiO layer on sapphire substrates provides the function of vertical alignment of the grown ZnO rods. By combining the sputtered Sn layer with spin-coated NiO to form a buffer bilayer, our best ZnO nanorods grown on NaOH-etched sapphire substrates had diameter of 110 $\pm$ 25 nm and length of 30 $\pm$ 10 $\mu$m. The green luminescence observed for rods with larger diameter is related to oxygen vacancies due to insufficient oxygen supply during the growth process.

## ACKNOWLEDGEMENT

The National Science Council is thanked for financial support through Grant No. 99-2221-E-011-045.

## REFERENCES

1. Z.L. Wang, *Mater. Sci. Eng. R* 64, 33 (2009).
2. Y.W. Heo, D.P. Norton, L.C. Tien, Y. Kwon, B.S. Kang, F. Ren, S.J. Pearton, and J.R. LaRoche, *Mater. Sci. Eng. R* 47, 1 (2004).
3. Z.L. Wang, L. Wang, X.Y. Kong, Y. Ding, P. Gao, W.L. Hughes, R. Yang, and Y. Zhang, *Adv. Funct. Mater.* 14, 943 (2004).
4. S. Xu, Y. Wei, M. Kirkham, J. Liu, W. Mai, D. Davidovic, R.L. Snyder, and Z.L. Wang, *J. Am. Chem. Soc.* 130, 14958 (2008).
5. T.Y. Liu, H.C. Liao, C.C. Lin, S.H. Hu, and S.Y. Chen, *Langmuir* 22, 5804 (2006).
6. H.J. Fan, B. Fuhrmann, R. Scholz, F. Syrowatka, A. Dadgar, A. Krost, and M. Zacharias, *J. Cryst. Growth* 287, 34 (2006).
7. X. Wang, C.J. Summers, and Z.L. Wang, *Nano Lett.* 4, 423 (2004).
8. D.S. Kim, R. Ji, H.J. Fan, F. Bertram, R. Scholz, A. Dadgar, K. Nielsch, A. Krost, J. Christen, U. Gosele, and M. Zacharias, *Small* 1, 76 (2007).
9. L. Wang, X. Zhang, S. Zhao, G. Zhou, Y. Zhou, and J. Qi, *Appl. Phys. Lett.* 86, 024108 (2005).
10. F.C. Taso, J.Y. Chen, C.H. Kuo, G.C. Chi, C.J. Pan, P.J. Huang, C.J. Tun, B.J. Pong, T.H. Hsueh, C.Y. Chang, S.J. Pearton, and F. Ren, *Appl. Phys. Lett.* 92, 203110 (2008).
11. P.X. Gao, Y. Ding, and Z.L. Wang, *Nano Lett.* 3, 1315 (2003).
12. Y. Ding, P.X. Gao, and Z.L. Wang, *J. Am. Chem. Soc.* 126, 2066 (2004).
13. J. Zhang, Y. Yang, F. Jiang, B. Xu, and J. Li, *J. Solid State Chem.* 178, 2804 (2005).
14. A. Umar, B. Karunagaran, E.K. Suh, and Y.B. Hahn, *Nanotechnology* 17, 4072 (2006).
15. S.Y. Li, C.Y. Lee, and T.Y. Tseng, *J. Cryst. Growth* 247, 357 (2003).
16. S.N. Cha, B.G. Song, J.E. Jang, J.E. Jung, I.T. Han, J.H. Ha, J.P. Hong, D.J. Kang, and J.M. Kim, *Nanotechnology* 19, 235601 (2008).
17. A. Umar, C. Ribeiro, A. Al-Hajry, Y. Masuda, and Y.B. Hahn, *J. Phys. Chem. C* 113, 14715 (2009).
18. S.T. Ho, K.C. Chen, H.A. Chen, H.Y. Lin, C.Y. Cheng, and H.N. Lin, *Chem. Mater.* 19, 4083 (2007).
19. F.H. Leiter, H.R. Alves, A. Hofstaetter, D.M. Hoffmann, and B.K. Meyer, *Phys. Status Solidi b* 226, R4 (2001).
20. X.L. Wu, G.G. Siu, C.L. Fu, and H.C. Ong, *Appl. Phys. Lett.* 78, 2285 (2001).
21. Y.M. Chiang, D. Birnie III, and W.D. Kingery, *Physical Ceramics: Principles for Ceramic Science and Engineering* (New York: Wiley, 1997), Chap. 2.
22. P.C. Chang, C.J. Chien, D. Stichtenoth, C. Ronning, and J.G. Lu, *Appl. Phys. Lett.* 90, 113101 (2007).
23. I. Shalish, H. Temkin, and V. Narayanamuti, *Phys. Rev. B* 69, 245401 (2004).
24. A.B. Djurišić and Y.H. Leung, *Small* 2, 944 (2006).